

# Comparative study between backstepping and backstepping sliding mode controller for suspension of vehicle with a magneto-rheological damper

Mohamed Belkacem<sup>1</sup>, Kadda Zemalache Meguenni<sup>1</sup>, Ismail Khalil Bousserhane<sup>2,3</sup>

<sup>1</sup>LDDE Laboratory, University of Sciences and Technology of Oran, Bir El Djir, Algeria

<sup>2</sup>ArchiPEL Lab, University of Tahri Mohamed, Bechar, Algeria

<sup>3</sup>Smart-Grid and Renewable Energies Laboratory, University of Tahri Mohamed, Bechar, Algeria

## Article Info

### Article history:

Received Oct 17, 2021

Revised Apr 1, 2022

Accepted Apr 16, 2022

### Keywords:

Backstepping control

Backstepping-sliding mode control

Magneto-rheological damper

Semi-active control

Sliding mode control

Vehicle suspension

## ABSTRACT

The Suspensions are among the important components of vehicles, providing comfort for passengers and protecting the chassis and freight. They are normally provided with dampers that mitigate these harmful and uncomfortable vibrations. This work aims at investigating the potential of the use of the Magneto-rheological Damper as a semi-active suspension for passenger vehicles to improve their ride dynamics and to, ensure their manipulability, and reduce unwanted vibrations levels. To achieve desired performances, a hybrid controller based on a backstepping-sliding mode control strategy is derived to increase the dynamic performance of the automotive suspension component and providing comfortable passenger traveling. Numerical simulation is used to test the efficiency of the proposed controller. The obtained results show that the proposed backstepping sliding mode controller is more efficient and robust against road profile excitation and external disturbances in comparison to a classical controller based on backstepping and sliding mode control.

*This is an open access article under the [CC BY-SA](https://creativecommons.org/licenses/by-sa/4.0/) license.*



## Corresponding Author:

Mohamed Belkacem

Department Electrical Engineering, LDDE Electric Drives Development Laboratory,

University of Sciences and Technology of Oran

Bir El Djir, Algeria

Email: belkacem\_mohamed03@yahoo.fr

## 1. INTRODUCTION

Nowadays, quality becomes very necessary for people around the world. Especially, comfort in vehicles, personal or public, is a priority concern for passengers therefore it is desirable to have a high-performance vehicle suspension system. Many vehicle components, such as suspension strut type, rolling center location and center of body weight, and steering system, might be potential elements for improving the performance of the suspension. Among these choices, suspension absorber studies are several and most active because improving performance of damper is the efficient choice to separate undesired vibrations generated due road profiles [1]. In the world of moving automobiles, passengers are not fully comfortable due to body vehicle vibration.

As a result, effective regulation of vehicle suspension vibrations is critical for improving driving comfort. In general, vehicle suspension is divided into three categories: active, semi-active and passive suspension [2]. Passive suspensions, which are often employed in traditional cars, are unable to increase driving comfort since their settings are fixed, and they may only perform well on specific road surfaces. Active suspension systems can improve riding comfort, but they always demand additional power.

Semi-active suspensions systems, on the other hand, feature changing damping coefficients or stiffness characteristics and do not require additional power sources. These suspension types are often defined by high-level technical professionals and also because of their relatively low frequency, changeable stiffness characteristics, and decreased suspension noise [3]. Semi-active suspensions with magneto-rheological (MR) dampers have emerged as the finest technical option for improving car suspensions just on road or the ride comfort. This seems to be due to benefits like the existence of a compromise in between attempting to control requirements for suspension damping for trying to drive comfort and ability to handle safety, the suitable control requirement for hysteresis as well as force saturation nonlinearities of MR dampers and highway vehicles uncertainty [4]. It has more advantages for obtaining desired performances compared with other suspension systems. It has, i.e., semi-active suspension, more advantages for obtaining desired performances compared with other suspension systems. For this reason, several researchers and academicals have taken more attention to study and develop suitable techniques and methods for semi-active vibrations attenuation and suppression. In recent years, experts and researchers have put forward many control strategies for vehicle suspension systems, such as PID control, optimal control, fuzzy control, neural network and adaptive control, sliding mode control [5]-[9].

Prabu *et al.* [6] have presented a pneumatic actuator control for vehicle suspension system using a classical PID controller. The pneumatic actuator model is modeled as the first-order system, and also the PID controller design was done using the Ziegler Nicolas tuning approach and optimum control, with comparison of the obtained results with passive suspension. Bao *et al.* [7] created an adaptive SMC controller based on fuzzy logic for the active suspension using air spring system. The suggested controller is intended in improving active suspension performance by using fuzzy control for dealing with the nonlinearity of system. For semi-active air suspension control, an adaptive technique based on neural networks and neural identifiers has been developed [8]. The strategy proposed in [8] used both neural networks and identifiers to compensate for the time-variation parameters and the nonlinearity of the air suspension system. Chang and Roschke [9] devised an alternate model of a MR damper in regards of a neural network.

A neural network approach with six neuronal inputs or one output to replicate the behavior of the MR dampers using the phenomenological model produced data. Wu and Griffin [10] created a relay on-off semi-active control strategy with an electro-rheological damper to reduce end-stop effects in suspension seats. Choi *et al.* [11] created a seat suspension system with such a skyhook control method and MR dampers. Suitable control techniques for MR systems, as well as design factors [12], have even been actively explored to improve the comfort performances with the accuracy and precision under extreme road excitations. The backstepping technique is widely used in nonlinear systems control and in suspension systems applications [13]-[19].

It can ensure worldwide tracking for such nonlinear systems class that can be transformed into the parameterized feedback form. Moreover, among novel strategies, the classic nonlinear controller using the SMC represents a strong tool for dealing with matched uncertainties and therefore is commonly employed for the nonlinear suspension systems [13], [17], [20]-[22]. The sliding mode controller's major shortcoming is the undesirable chattering phenomena, which can stimulate high-frequency response thus contribute to the instability. Many techniques, such as the combining of backstepping with sliding mode control, have been offered to avoid the issue of chattering. These nonlinear controls are intended to increase vehicle agility and the driving comfort [13]-[22]. The goal of this research is to create and investigate the vibration signals of a MR suspension under various road circumstances employing three nonlinear control systems: backstepping strategy, slide mode control, and back-stepping-sliding controlling. The remainder of the study is arranged as follows: section 2 develops a MR damper behavior and model. Section 3 includes a quarter car model for said semi-active suspension system. Section 4 develops several control techniques for the semi-active suspension control based upon backstepping, SMC, and backstepping-SMC design to negate the influence of unknown road roughness on the vehicles. The obtained simulation results of these controllers and comparisons are discussed in the section 5. Finally, the results are drawn in section 6.

## 2. MATHEMATICMODEL OF THE MAGNETO-RHEOLOGICAL DAMPER

Today, MR dampers have been used for several times to reduce the vibration picks in dynamic systems including active suspension control. In several practices cases, it has been verified that undesired vibrations of systems can be reduced using MR dampers with known theoretical control strategies [2], [23]-[26]. This semi-active device behaves similarly to a hydraulic damper, with the exception that its fluid can modify its yield point when such an external magnetic field. Ultimately, MR dampers are strong devices that combine the benefits of passive components with the advantages of active control [24], [27], [28].

Figure 1 depicts the MR damper arrangement. The damping device is essentially made up of a hydraulic cylinder containing magnetizable micro particles flowing in oil-like fluids. A tiny opening on one

side of the piston allows fluid to pass through. Once the application of magnetic field is done, the particles become polarized and, in a few milliseconds, transition to the semi-solid phase with a high flow resistance. The changing magnetic field causes the viscous effects to become adjustable, and as a result, damping forces may be created to dampen the existing oscillations [24]-[26].

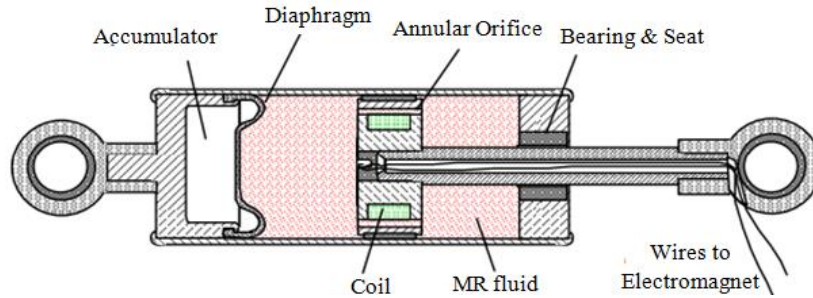


Figure 1. The basic configuration of the MR damper

The mathematic equations of the damper can be used to describe the applied voltage or current or to the MR circuit with the produced damping force. Several scholars have constructed statistical models to describe the hysteretic behavior of MR damper in the research. Figure 2 depicts the well-known enhanced Bouc–Wen model, which describes the characteristics of MR dampers [29]-[31]. Spencer *et al.* [29] created a phenomenological framework wherein the force of the MR damper is described as a function of the spring stiffness, accumulation stiffness, viscous damping at a low velocity, and damping or stiffness at high speeds. The following is an expression for the forces generated by the MR dampers using the generalized Bouc-Wen model: [12], [14], [29]-[31].

$$f_{MR} = c_1 \dot{y} + k_1(x - x_0) \tag{1}$$

$$c_1 \dot{y} = c_0(\dot{x} - \dot{y}) + k_0(x - y) + \alpha z \tag{2}$$

$$\dot{z} = -\gamma|\dot{x} - \dot{y}|z|z|^{n-1} - \beta(\dot{x} - \dot{y})|z|^n + A(\dot{x} - \dot{y}) \tag{3}$$

$$\dot{y} = \frac{1}{c_0+c_1} [\alpha z + c_0 \dot{x} + k_0(x + y)] \tag{4}$$

Where  $x$ , and  $f_{MR}$  indicate the damper's displacement, speed, supply voltage, and produced force, respectively,  $z$  is an evolving variable that which characterizes the hysteresis behavior of the MR damper force versus the damper's movement and velocity. The hysteresis loop's form and size are described by the parameters, and  $A$ . The device's extra parameters may be represented as a function of applied voltage as follows [29]-[31]:

$$\alpha = \alpha_a + \alpha_b u ; c_1 = c_{1a} + c_{1b} u ; c_0 = c_{0a} + c_{0b} u \tag{5}$$

where  $u$  is a variable that defines the dynamic of the system given by:

$$\dot{u} = -\tau_f(u - v) \tag{6}$$

where  $v$  is the control voltage supply at terminals of the driver and  $\tau_f$  denotes the first-order filter time constant.

Parameters of the mangnetorheological damper model adopted are given as:  
 $c_{0a} = 7.84N \cdot s/cm ; c_{0b} = 18.03N \cdot s/cm ; k_0 = 36.1N/cm ; k_1 = 8.4N/cm ; c_{1a} = 146.49N \cdot s/cm ;$   
 $c_{1b} = 34.622N \cdot s/cm ; \alpha_a = 124.41N/cm ; \alpha_b = 384.3N/cm ; \gamma = 136.32cm^{-2} ;$   
 $\beta = 205.9020cm^{-2} ; A = 251 ; n = 2 ; \eta = 190s^{-1} ; x_0 = 09.08cm.$

A sinusoidal signals displacement with the amplitude of 1.25cm and 1.5 Hz frequency is performed for varied supplied input voltages to validate the behavior and hysteresis features of the proposed MR damper type (0, 0.5, 0.75, 1, and 1.25 V). Figure 3 depict the produced force's temporal response, the pressure against MR damping displacement, as well as force-velocity hysteresis. The various plotted charts of the produced force clearly show the hysteresis behavior of the MR damper in between time Figure 3(a) and velocity  $x$  and the damper force  $f_{MR}$  as shown in Figure 3(b), and the non-linearity characteristics of  $f_{MR}$  according to  $x$  variation is remarkable (see Figure 3(c)).

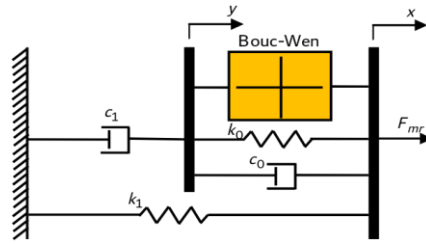


Figure 2. The schematic representation of the magnetorheological damper according to the Bouc-Wen model

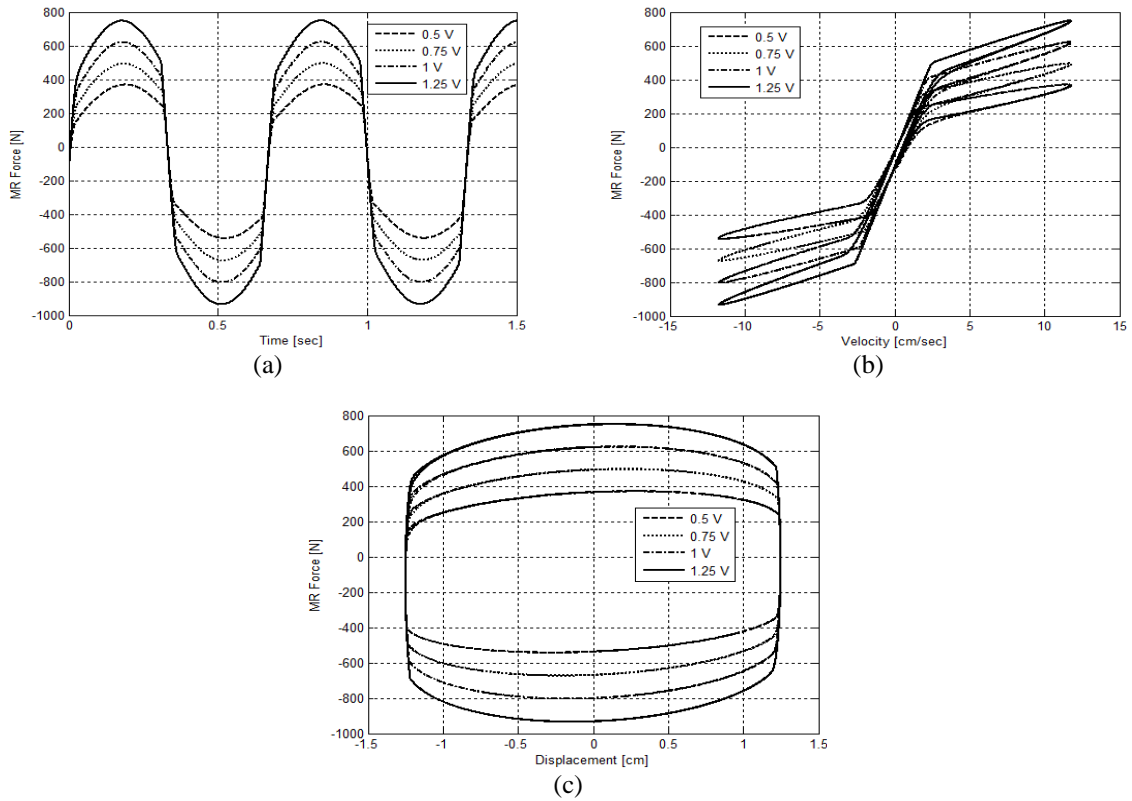


Figure 3. Produced force of MR damper model on the (a) MR force-time, (b) MR force-velocity and (c) MR force-displacement

### 3. DYNAMIC MODEL OF MR QUARTER-VEHICLE SUSPENSION SYSTEM

Despite the fact that the genuine suspension may be treated in a way more sophisticated, the suggested model simplifies the complicated geometry of the suspension structure [32]. To investigate the robustness of the suspension control strategy we suppose a quarter vehicle system as shown in Figure 4 [13], [20], [30]. It is a basic structural model since it consists primarily of two subsystems: the wheel mass which represents tyre subsystem and also the body mass which represents the subsystem of suspension. These two subsystems are connected between them via elastic and dissipative elements and are subjected to external disturbances, which are represented by the road profile. From the mechanical model depicted in the Figure 4, the mathematic equations of the 1/4-vehicle model are written as follows [13], [20], [30]:

$$m_s \ddot{z}_s = k_s(z_u - z_s) + C_s(\dot{z}_u - \dot{z}_s) - F_{mr} \tag{7}$$

$$m_u \ddot{z}_u = k_u(z_r - z_u) - k_s(z_u - z_s) - C_s(\dot{z}_u - \dot{z}_s) - F_{mr}$$

with  $z_s, z_u$  and  $z_r$  denote the vertical displacement of the sprung mass, the unsprung mass and the external disturbance due to the road profile, respectively.  $F_{mr}$  the force produced by the MR damper;  $m_s$  and  $m_u$  respectively are the car body and the wheel assembly masses.  $k_s$  and  $k_u$  represent the stiffness of the suspension and the stiffness of tire.  $C_s$  is the total damping constant of the suspension. We define the state variables  $x$ , the input force vector  $u$  and the road profile disturbance  $W$  as follows:

$$x = [z_s \quad \dot{z}_s \quad z_u \quad \dot{z}_u]^T = [x_1 \quad x_2 \quad x_3 \quad x_4]^T,$$

$$u = [F_{mr}], W = [z_r]$$

then, the 1/4-vehicle model can be expressed in state-space as (8).

$$\dot{x} = Ax + Bu + DW \tag{8}$$

Where:

$$A = \begin{bmatrix} 0 & 1 & 0 & 0 \\ -\frac{k_s}{m_s} & -\frac{C_s}{m_s} & \frac{k_s}{m_s} & \frac{C_s}{m_s} \\ 0 & 0 & 0 & 1 \\ -\frac{k_s}{m_u} & \frac{C_s}{m_u} & -\frac{k_s+k_u}{m_u} & -\frac{C_s}{m_u} \end{bmatrix}, B = \begin{bmatrix} 0 \\ \frac{1}{m_s} \\ 0 \\ -\frac{1}{m_u} \end{bmatrix}, D = \begin{bmatrix} 0 \\ 0 \\ 0 \\ -\frac{k_u}{m_u} \end{bmatrix}$$

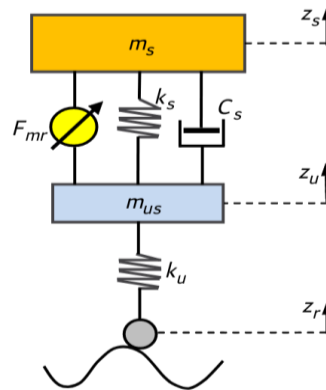


Figure 4. Quarter-vehicle model with MR damper

#### 4. CONTROL ALGORITHMS OF VEHICLE SUSPENSION DYNAMICS

This section proposes semi-active controls of the vehicle suspension dynamics depending on multiple nonlinear control schemes. There are three forms of nonlinear control formed: backstepping control, slide mode control, as well as a hybridation backstepping-sliding mode control scheme. All of these kinds of controls are dependent on the Lyapunov stability criteria, which will be shown in the next subsections.

##### 4.1. Vehicle suspension control using backstepping strategy

Backstepping seems to be a systematic and recursive nonlinear feedback control design approach ideal for the wide category of feedback nonlinear systems. This technique ensures global pursuit for such nonlinear systems category that can be transformed into parametric-strict survey form [13], [14], [33]-[35]. The control law's backstepping technique relies on a recursive selection of some relevant functions using system states as virtual-control inputs for the under dimension subsystems. Each step of the backstepping startegy generates a virtual-control signal, which is expressed in relation of the previous design phases virtual-control designs. When technique steps are completed, a feedback disposition for the actual control input signal is produced, which meets the desired design target by summing the Lyapunov activities connected with each individual design phase [13], [14],[33]-[35].

- Step 1: If we opt to reduce the suspension travel, the oscillating subsystem problem will remain unaddressed. Because we know that proper controlled variables can help to avoid unpredictable zero dynamic features, the regulated output is set to be [36]:

$$e_1 = x_1 - \tilde{x}_3 \tag{9}$$

where  $x_1$  is the displacement of car body,  $\tilde{x}_3$  is a filtered version of the wheel displacement  $x_3$ :

$$\tilde{x}_3 = \frac{\varepsilon}{s+\varepsilon} x_3 \quad (10)$$

where  $\varepsilon$  is a positive constant.

$$\begin{aligned} \dot{e}_1 &= \dot{x}_1 - \dot{\tilde{x}}_3 \\ &= x_2 - \varepsilon(x_3 - \tilde{x}_3) \\ &= x_2 + \varepsilon(x_1 - x_3) - \varepsilon e_1 \end{aligned} \quad (11)$$

Because of that the error  $e_1$  must be equal to zero, state variable  $x_2$  is taken as the virtual control to make the first subsystem stable. In order to compute the stabilizing function, we defined the following Lyapunov function as:

$$V = \frac{1}{2} e_1^2 \quad (12)$$

We differentiate to get:

$$\begin{aligned} \dot{V} &= e_1 \dot{e}_1 \\ &= e_1(x_2 + \varepsilon(x_1 - x_3) - \varepsilon e_1) \\ &= -K_1 e_1^2 + (K_1 e_1 + x_2 + \varepsilon(x_1 - x_3) - \varepsilon e_1) \end{aligned} \quad (13)$$

where,  $K_1$  is constant gain. The error is achieved if we define stabilization function as:

$$\alpha_1 = -K_1 e_1 - \varepsilon(x_1 - x_3) + \varepsilon e_1 \quad (14)$$

with  $\alpha_1 = x_2^{ref}$  and  $K_1 > 0$  a positive design constant.

By substituting (14) and (11) into (13) yields

$$\dot{V}_1 = -K_1 e_1^2 \quad (15)$$

- Step 2: now, in the next step we try to make the virtual control  $x_2^{ref}$  as desired. So, we define the following error signal

$$e_2 = x_2 - \alpha_1 \quad (16)$$

and the error equation is:

$$\dot{e}_1 = -(K_1 + \varepsilon)e_1 + e_2 \quad (17)$$

$$\begin{aligned} \dot{e}_2 &= \dot{x}_2 - \dot{\alpha}_1 \\ &= \frac{1}{m_s} [k_s(x_1 - x_3) - c_s(x_2 - x_4) - F_a - (K_1(-K_1 + \varepsilon)e_1 + e_2) - \varepsilon(x_2 - x_4)] \end{aligned} \quad (18)$$

To determine the stabilizing function, the augmented Lyapunov function is defined as:

$$V = \frac{1}{2} e_1^2 + \frac{1}{2} e_2^2 \quad (19)$$

So, its derivative is defined as follow:

$$\begin{aligned} \dot{V} &= e_1 \dot{e}_1 + e_2 \dot{e}_2 = e_1(-(K_1 + \varepsilon)e_1) \\ &\quad + e_2 \left( \frac{1}{m_s} [k_s(x_1 - x_3) - c_s(x_2 - x_4) - F_a - (K_1(-K_1 + \varepsilon)e_1 + e_2) - \varepsilon(x_2 - x_4)] \right) \end{aligned} \quad (20)$$

The control tracking is achieved if one defines the following stabilizing function:

$$F_a = m_s(-(K_2 + K_1)e_2 + (K_2^2 - 1 + K_1\varepsilon)e_1) + k_s(x_1 - x_3) + c_s(x_2 - x_4) \tag{21}$$

where  $F_a$  denotes the desired active force which must be produced by the MR damper (i.e.  $F_a = F_{mr}$ ).  $K_2$  is a positive constant, by substituting (21) into (20) yields.

$$\dot{V}_1 = -(K_1 + \varepsilon)e_1^2 - K_2e_2^2 \tag{22}$$

Thus, the system is asymptotically stable. The system is simulated in the Simulink as shown in Figure 5.

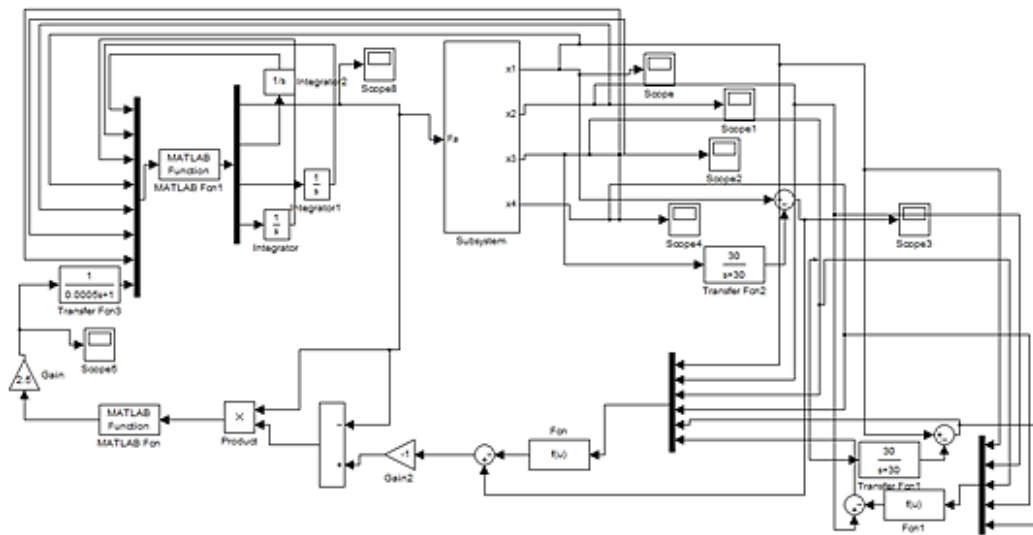


Figure 5. Simulation of a quarter vehicle suspension model using MR damper with backstepping control

**4.2. Vehicle suspension control using sliding mode control**

Many research studies have used the variable structure with the sliding mode, or sliding mode control, in the previous decades for non - linear control processes [7], [13], [17], [20]-[22], [37]-[39]. The sliding mode controller (SMC) seems to be a non-linear control mechanism that modifies the dynamics of a non-linear system, causing it to slide. The SMC is widely renowned for its resilience, high stability, and straightforward implementation [40]-[42]. The characteristic of the sliding mode relies on directing a system's state trajectory toward this sliding surface and directing it to switch across it to the equilibrium point using proper switching logic, resulting in the sliding phenomena. The benefits of SMC control are numerous and considerable, including improved accuracy, a very rapid reaction time, and, most importantly, resilience [43], [44]. In general, the sliding mode control design procedure can divide in two steps. The first step of SMC design involves the selection of the sliding surface (sometimes referred to the switching surface or switching manifold  $S(x) = 0$ ) in the state space where the control undergoes discontinuities [13], [20], [21]. This sliding surface is chosen to simulate the required closed loop performances.

Insecond phase, the control rule should be devised such that such system's state trajectory are driven toward and remain on the sliding surface. The reaching phase refers to the system state trajectory before to reaching the sliding surface. The generic expression of Slotine and Li's sliding surface is calculated by:

$$S(x) = \left(\frac{d}{dt} + \lambda\right)^{n-1} e(x) \tag{23}$$

where  $e(x) = x_d - x$  denotes the tracking error,  $\lambda$  is a positive constant,  $x$  is the variable state.

The sliding-mode control law  $u$  is consisting of two components. One is the equivalent control  $u_{eq}$  and the other is switching control input  $u_s$ , i.e. [7], [20].

$$u = u_{eq} + u_s \tag{24}$$

where  $u_{eq}$  is called equivalent control which dictates the motion of the state trajectory along the sliding surface and  $\lambda$  is known as switching control part which is given in the basic form as:

$$u_s = k \cdot \text{sgn}(S(x)) \quad (25)$$

where  $k$  is a positive constant.

The control input should be designed such that the following sliding condition is satisfied:

$$S(x) \cdot \dot{S}(x) < 0 \quad (26)$$

using a sign function often causes chattering in practice. Among the solution of this problem is to introduce a boundary layer around the switching surface, and the switching component is become as:

$$u_s = k \cdot \text{sat}\left(\frac{S(x)}{\xi}\right) \quad (27)$$

where  $\text{sat}(x)$  is the saturation function defined as (28).

$$\text{sat}\left(\frac{S(x)}{\xi}\right) = \begin{cases} \frac{S(x)}{\xi} & \left| \frac{S(x)}{\xi} \right| \leq \xi \\ \text{sgn}\left(\frac{S(x)}{\xi}\right) & \left| \frac{S(x)}{\xi} \right| > \xi \end{cases} \quad (28)$$

Where  $\xi$  denotes the boundary layer thickness around the sliding surface. The conventional SMC uses a control law with large control gains and can produce some drawbacks associated with large control chattering. The control-input chattering is undesired and it may excite high-frequency response and lead to instability.

#### 4.2.1. Sliding mode speed controller design

The goal of the control technique is to create a nonlinear control system based on sliding - mode that achieves high accuracy and precision tracking under uncertainties and disturbances. The following stages are included in the design of the proposed sliding - mode for the semi-active suspensions control. The following is the definition of error tracking:

$$e = (x_1 - \tilde{x}_3)$$

Then, the general sliding surface is given by:

$$S = \frac{d}{dt}(x_1 - \tilde{x}_3) + \lambda \cdot (x_1 - \tilde{x}_3) \quad (29)$$

a sliding condition must be established in order for the state to travel toward and achieve the sliding surface. The suggested sliding condition is [20], [21]:

$$S \cdot \dot{S} \leq -\eta \cdot |S| \quad (30)$$

where  $\eta$  is a positive constant.

The damping force is calculated by deriving (29) since it forces trajectory to point toward this sliding surface. The systems trajectories, in particularly, adhere to the surface then on surface, i.e.

$$S = 0 \quad (31)$$

From (28) and (29):

$$\begin{aligned} \dot{S} &= \ddot{e} + \lambda \dot{e} \\ &= k_s x_1 + (C_s - \lambda m_s m_{us} / (m_s + m_{us})) x_2 \\ &\quad - (k_s + k_{us} m_s / (m_s + m_{us})) x_3 + (C_s - \lambda m_s m_{us} / (m_s + m_{us})) x_4 \\ &\quad + k_{us} x_r m_s / (m_s + m_{us}) - F_a \end{aligned} \quad (32)$$



The best approximation for the desired damping force  $F_a$ , a control law should achieve  $\dot{S} = 0$  thus;

$$F_a^{equ} = k_s x_1 + (C_s - \lambda m_s m_{us} / (m_s + m_{us})) x_2 - (k_s + k_{us} m_s / (m_s + m_{us})) x_3 + (C_s - \lambda m_s m_{us} / (m_s + m_{us})) x_4 + k_{us} x_r m_s / (m_s + m_{us}) \tag{33}$$

In order to satisfy sliding condition, a term discontinuous across the surface is added to the equivalent control  $F_a^{equ}$ , then the desired control force  $F_a$  can be expressed as:

$$F_a = F_a^{equ} + k \cdot \text{sat} \left( \frac{S}{\xi} \right) \tag{34}$$

with  $k > 0$ . The system is simulated in the Simulink as shown in Figure 6.

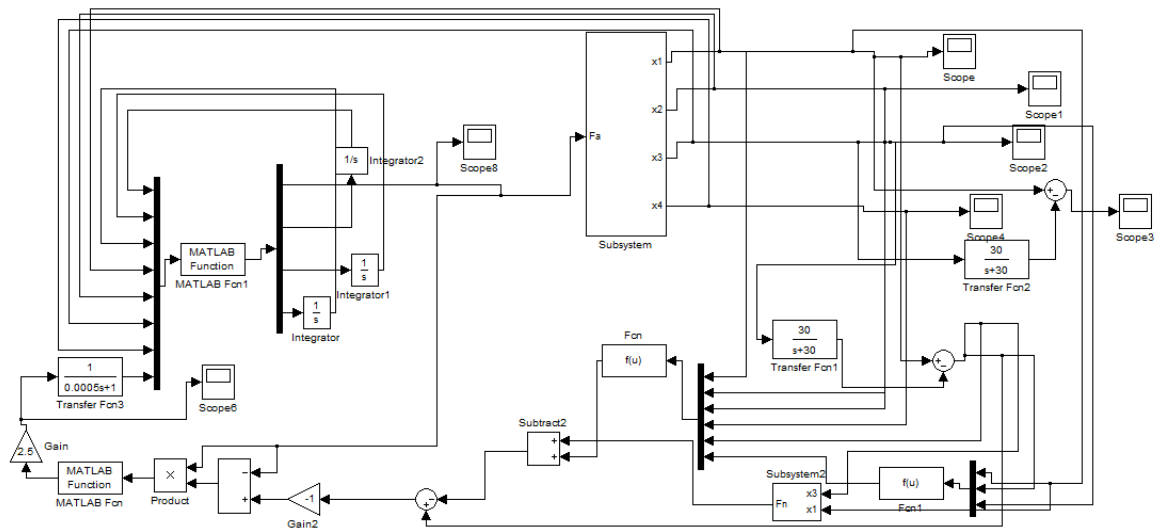


Figure 6. Simulation of a quarter vehicle suspension model using MR damper with sliding mode control

**4.3. The hybrid controller backstepping-sliding mode design**

The control goal is to construct a backstepping sliding-mode control [45]-[49] system to monitor the reference trajectory for the outputs of the vehicle suspension illustrated in (9). The suggested backstepping sliding-mode control system is intended to meet the goal of automobile body displacement tracking. This controller's output is really the reference force which must be delivered by the MR damper, and it is discussed in:

- Step 1: The tracking error is chosen as shown in section 4.1:

$$e_1 = x_1 - \tilde{x}_3 \tag{35}$$

the derivative of  $e_1$  is computed as:

$$\begin{aligned} \dot{e}_1 &= \dot{x}_1 - \dot{\tilde{x}}_3 \\ &= x_2 - \varepsilon \cdot (x_3 - \tilde{x}_3) \\ &= x_2 + \varepsilon \cdot (x_1 - x_3) - \varepsilon \cdot e_1 \end{aligned} \tag{36}$$

the first Lyapunov function is chosen as:

$$V_1 = \frac{1}{2} e_1^2 \tag{37}$$

define the first virtual control variable,

$$x_{2ref} = \varphi_1 = -K_1 \cdot e_2 - \varepsilon \cdot (x_1 - x_3) \tag{38}$$

then, the derivative of  $V_1$  is:

$$\begin{aligned} \dot{V}_1 &= e_1 \dot{e}_1 = e_1(x_2 - \varepsilon \cdot x_3 + \varepsilon \cdot x_1 - \varepsilon \cdot e_1) \\ &= -(K_1 + \varepsilon) \cdot e_1^2 < 0 \end{aligned} \tag{39}$$

with  $K_1$  is a positive design gain,

- Step 2: We define a sliding surface

$$S = x_2 - \varphi_1 \tag{40}$$

So, it is easy to find the following expression:

$$\dot{e}_1 = -(K_1 + \varepsilon)e_1 + S \tag{41}$$

The second Lyapunov function is chosen as:

$$V_2 = V_1 + \frac{1}{2}S^2 \tag{42}$$

where  $S$  is the sliding surface. So, the derivative of  $V_2$  is expressed as follow

$$\dot{V}_2 = \dot{V}_1 + S \cdot \dot{S} \tag{43}$$

To ensure that  $\dot{V}_2 < 0$  we take  $\dot{S} = -K_f \operatorname{sgn}(S) - K \cdot S$ ; with  $K_f$  and  $K$  are positive gains.

Differentiating the (40) which yields.

$$\dot{S} = \dot{x}_2 - \dot{\varphi}_1 = \frac{1}{m_s}(k_s(x_3 - x_1) + C_s(x_4 - x_2) + F_a) - \dot{\varphi}_1 \tag{44}$$

Finally, the control law resulting by sliding mode is of the form:

$$F_a = m_s(-K_f \operatorname{sgn}(S) - K \cdot S) - k_s(x_3 - x_1) - C_s(x_4 - x_2) + m_s \dot{\varphi}_1 \tag{45}$$

then,

$$\dot{V}_2 < 0 \tag{46}$$

therefore,  $e_1$  and  $e_2$  will converge to zero. The stability of the proposed backstepping sliding mode control system can be guaranteed. The system is simulated in the Simulink as shown in Figure 7.

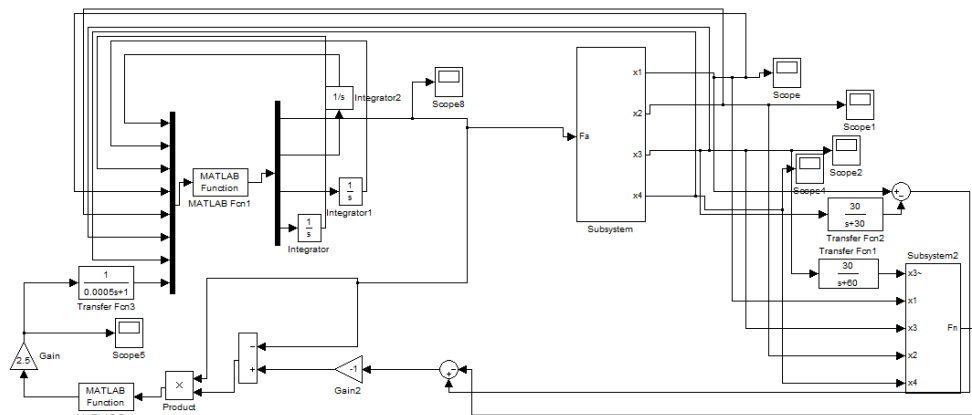


Figure 7. Simulation of a quarter vehicle suspension model using MR damper with hybrid controller backstepping-sliding mode

**4.4. Semi-active control system**

The semi-active control system consists of two controllers. The first one is the system controller which produces the appropriate active damping force ( $F_a$ ) corresponding to the suspension responses due to the road profile excitation, while the role of the second controller is the adaptation of the input voltage level which keeps the MR damper force on the desired active damping force ( $F_a$ ). In this paper, the semi-active controller is essentially composed of backstepping controller, sliding mode control or backstepping sliding mode control (system controller) and a function unit which used for converting the desired control force to an input control voltage (damper controller). The usually adopted algorithm for the conversion of the force to a adjusted voltage for the conversion is a clipping algorithm [29], [32]:

$$v = v\{(F_a - F_{mr}) \cdot F_{mr}\}_{max} \tag{47}$$

where  $v_{max}$  is the maximum applied voltage,  $H\{\cdot\}$  is a Heaviside step function,  $F_{MR}$  is a measured MR damper force, and  $F_{mr}$  denotes the desired active control force produced by the system controller (backstepping control/SMC or Backstepping-sliding mode control (B-SMC)).

The structure of the closed-loop semi-active controller using the proposed nonlinear controllers for vehicle suspension with an MR damper is depicted in Figure 8. In the first step, the actions specified control force is computed using one of the nonlinear controllers based on vehicle suspension system outputs. Because the control input  $v$  directly represents the damping force  $f_{MR}$ , the Heaviside step function is employed to adjust the input voltage control according to the desired damping function and the real force realized by the MR damper.

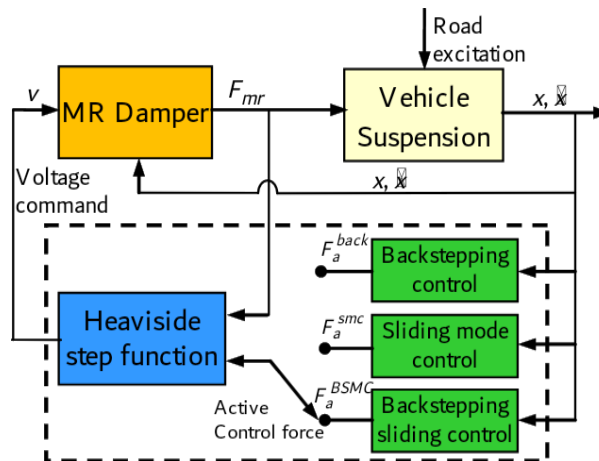


Figure 8. The block diagram of a semi-active control system for vehicle suspension with MR damper uses the proposed nonlinear controllers

**5. SIMULATION RESULTS**

The quarter vehicles suspension structure is subjected to two types of road stimulation in order to assess the performance of the semi-active control with MR damper utilising the suggested nonlinear controllers. The bump in Figure 9(a) is the very first stimulation signal studied, and it is typically used to highlight dynamic response properties. The bump excitation is described by:

$$\begin{cases} z_r = A_m(1 - \cos(\omega t)) & 1 \leq t \leq 2 \\ z_r = 0 & \text{otherwise} \end{cases} \tag{48}$$

where  $\omega = 2\pi f$  denotes the frequency [rad/sec],  $A_m$  represents the bump height. The second road excitation tested is a step excitation in Figure 9(b) with an amplitude of  $0.2\text{ m}$ . These types of road excitations, illustrated in Figures 9(a) and 9(b) are applied to the vehicle suspension system as shown in Figure 8.

The following are the different parameters of the suggested adaptive sliding mode control that are regarded to produce high transient control stability and performance which are used for control loop:  $K_1 = 450$ ,  $K_2 = 15$ ,  $k = 12.5$ ,  $\xi = 0.05$ ,  $K_f = 7.5$ ,  $K = 2.5$ . The simulation parameter values of the vehicle suspension system are listed in Table 1.

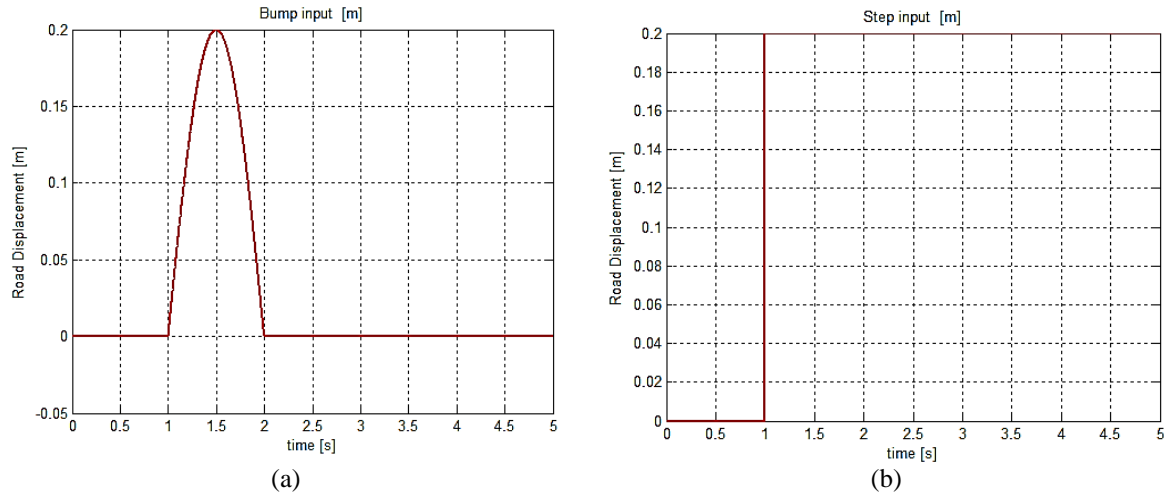


Figure 9. Type of road excitations for simulation: (a) bump excitation and (b) step excitation

Table 1. Parameter numerical value of the quarter vehicle model

Symbol	Value	Description
$m_s$	315 kg	Sprung mass
$m_{us}$	37.5 kg	Unsprung mass
$K_s$	29500N/m	Suspension linearised stiffness
$C_s$	15 00N/m/s	Suspension linearised damping
$K_{us}$	210000N/m	Tyrestiffness

Figures 10(a)-(c) show the vertical displacement of an automobile body, acceleration of the sprung mass, and vertical displacement of the unsprung mass utilizing nonlinear controllers (backstepping control, sliding mode control, and backstepping-sliding control) for the bump road excitation. In contrast to the passive suspension, the outcomes shown in Figure 10 clearly demonstrate that using the suggested semi-active suspension system can obtain excellent performances in which the undesired vibrations due to road excitation have really been clearly diminished (lower amplitude for the vehicle acceleration, vehicle displacement, and wheel displacement). It definitely demonstrates the efficacy and durability of the recommended semi-active vehicle suspension control with MR dampers for induced vibrations mitigation.

Figures 11 (a)-(c) depicts the acquired results for vertically vehicle displacement, vertical accelerating of sprung mass, and wheels vertical displacement for step road excitation. According to simulation results, the systems displacement and accelerating responses are significantly decreased, and the steady-state duration of controller system responds is significantly quicker than the passive system. We see that the displacements as well as accelerations have been reduced significantly, confirming that the performance have been enhanced. Thus, it can be stated that high passenger comfort may be gained by minimizing body movement as much as feasible, as demonstrated by the nonlinear semi-active control. Based on the dynamic response characteristics, we can conclude that the suggested semi-active control with the MR damper based on backstepping-sliding mode approach outperforms the other investigated nonlinear controls (i.e. Sliding mode control and backstepping control).

Figure 12 depicts the applied voltage level to the semi-active suspension's MR damper. We can see that the Voltage level is constantly switching between zero and the maximum voltage based on differences between produced forces and clipped-control. Figure 13 depicts a contrast of the real damping force, desired damping force, and active force. Figure 13 means that the actual damping forces generated by the MR dampers can following the reference damping force with precision and decrease tracking error, demonstrating the usefulness of the clipper optimum control utilised in damping force control.

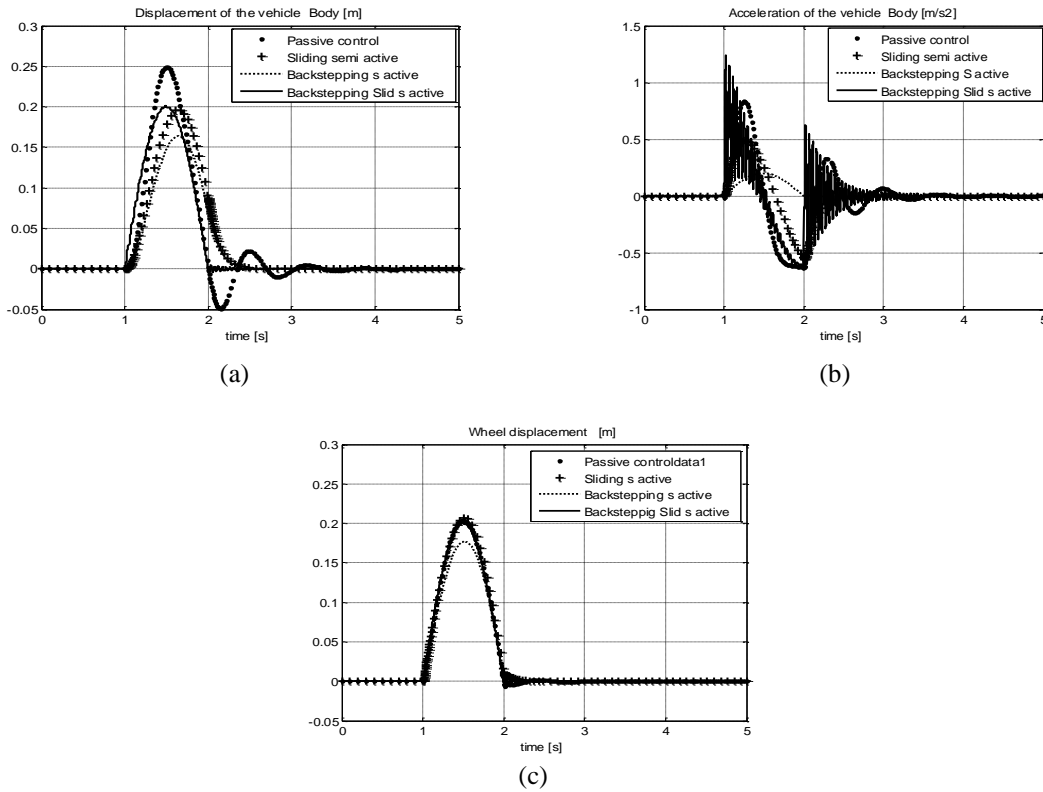


Figure 10. Simulation findings for semi-active vehicle suspension control with MR damper under bump road stimulation: (a) vehicle body displacement responses (b) vehicle body accelerating responses, and (c) wheel displacement responses

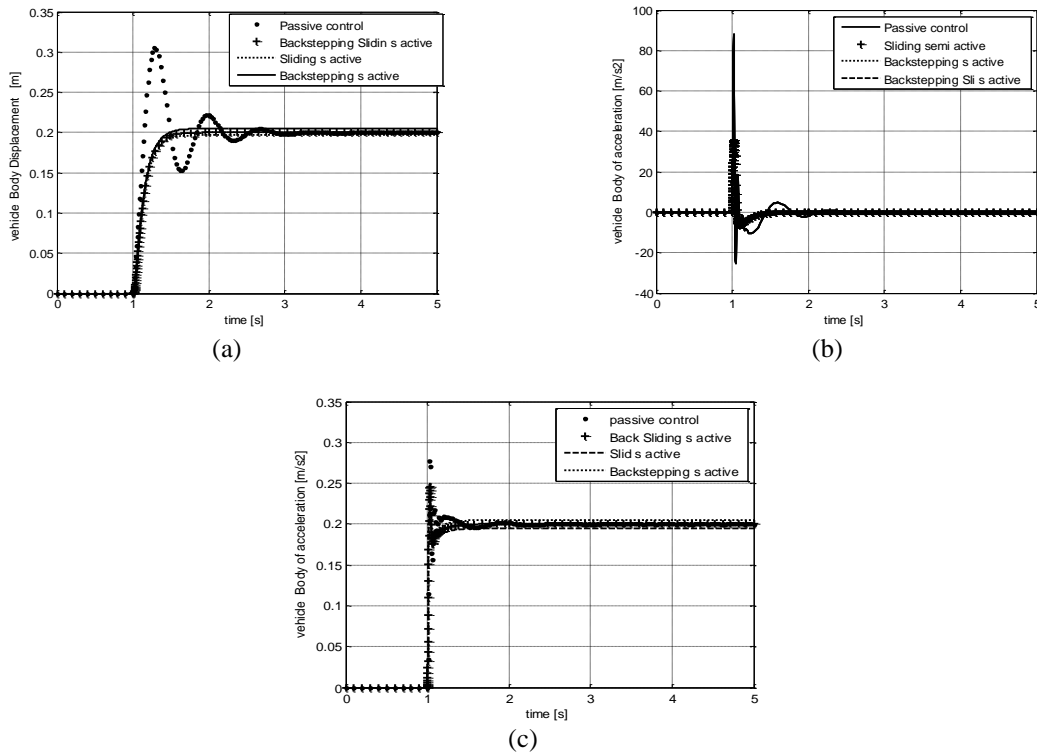


Figure 11. Simulation findings for semi-active vehicle suspension control with MR damper under step road stimulation: (a) vehicles body displacement reactions, (b) vehicle body accelerating responses, and (c) wheel displacement reactions

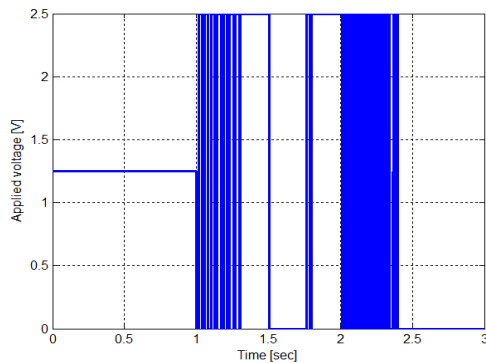


Figure 12. depicts the input voltage provided to the MR damping driver of semi-active control using a back stepping-sliding mode technique for a bumpy road excitation testing

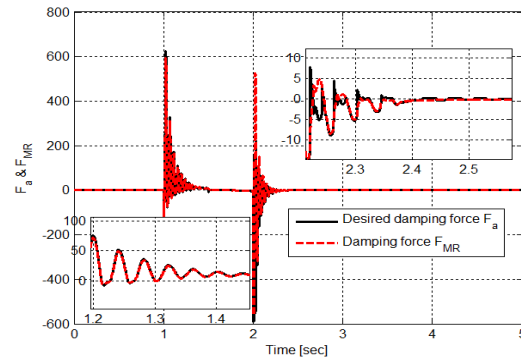


Figure 13. A comparison of the real damp force and also the target damping force for a bump roadway excitation test using a semi-active power based on a backstepping-sliding mode technique

## 6. CONCLUSION

To reduce undesirable vibrations caused by road irregularity, a semi-active control based on a clipper optimum control method for MR damper is suggested in this study for a vehicle suspension system. To improve the performance of the vehicle MR damper suspension system, the suggested control strategy includes the creation of a classic control scheme, a back stepping control approach, and a hybrid back stepping-sliding phase controller. The nonlinear control techniques and the clipper control algorithm are used to generate the active damping power and the MR damper driver's modified input voltage. In the first stage, a generalized model of the MR damper based on modified Bouc-Wen model is provided. Next, for a semi-active controlling, 3 types of nonlinear control methods, backstepping, slide mode, and backstepping-sliding authority, are created and used to the quarter-vehicle rear suspension.

Numerical methods utilizing MATLAB/Simulink programs are used to evaluate the effectiveness of the suggested control techniques for various forms of road excitations. It has been quantitatively demonstrated that the semi-active controller performs well and can significantly minimize or suppress the produced vibrations. Moreover, we observe that the hybrid backstepping-sliding mode controlling is more durable and effective than the other nonlinear systems. Thus, the obtained findings indicate that proposed control mechanisms connected with the chosen MR suspension system may greatly increase passenger comfort.

## REFERENCES




- [1] Dal-Seong Yoon, Gi-Woo Kim, Seung-Bok Choi, "Response time of magnetorheological dampers to current inputs in a semi-active suspension system: Modeling, control and sensitivity analysis," *Mechanical Systems and Signal Processing*, vol. 146, p. 1069992021, doi: 10.1016/j.ymssp.2020.106999.
- [2] F. Lam, C. Y. Lai, and W. H. Liao, "Automobile Suspension Systems with MR Fluid Dampers," Technical Report Department of Mechanical and Automation Engineering, The Chinese University of Hon Hong, 2002.
- [3] L. Q. Sun, Z. X. Li, X. Xu, "Control and Test of Semi - active Air Suspension Damped Sliding Mode Variable Structure," *Journal of Jiangsu University Natural Science Edition*, vol. 35, no. 6, pp. 621-626, 2014.
- [4] D. L. Margolis, "A procedure for comparing passive, active, and semi-active approaches to vibration isolation," *Journal, of the Franklin Institute*, vol. 315, no. 4, pp. 225-238, 1983, doi:10.1016-0016-0032(83)90074-1.
- [5] Y. S. Zhao, Z F Liu, L G Cai, W Yang, "Fuzzy Adaptive Sliding Mode Control of Active Air Suspension Based on Model Reference," *Mechanical Science and Technology*, vol.29, no. 1, pp. 12-16, 2010.
- [6] K. Prabu, J. Jancirani, J. Dennie, and B. Arun, "Vibrational control of air suspension system using PID controller," *Journal of Vibro Engineering*, vol. 15, no. 1, pp. 132-138. 2013.
- [7] W.-N. Bao, L.-P. Chen, Y.-Q. Zhang, and Y.-S. Zhao, "Fuzzy adaptive sliding mode controller for an airSpring active suspension," *International Journal of Automotive Technology*, vol. 13, pp. 1057-1065, 2012, doi:10.1007/s12239-012-0108-2.
- [8] H. Wang, "Neural Network Adaptive Control for Semi-active Air Suspension," *Transactions of the Chinese Society for Agricultural Machinery*, vol.37, no. 1, pp. 28-31, 2006.
- [9] C. C. Chang and P. Roschke, "Neural network modeling of a magnetorheological damper," *Journal of Intelligent Material Systems and Structures*, vol. 9, pp. 755-764, 1998, doi:10.1177/1045389X9800900908.
- [10] X. Wu and M. J. Griffin, "A semi-active control policy to reduce the occurrence and severity of end-stopimpacts in a suspension seat with an electrorheological fluid damper," *Journal of Sound and Vibration*, vol. 203, no. 5, pp. 781-793, 1997, doi:10.1006/jsvi.1996.0901.
- [11] S. B. Choi, M. H. Nam, and B. K. Lee, "Vibration control of a MR seat damper forcommercial vehicles," *Journal of Intelligent Material Systems and Structures*, vol. 11, no. 12, pp. 936-944, 2000, doi: 10.1106/AERG-3QKV-31V8-F250.

- [12] S.B. Choi, W. Li, M. Yu, H. Du, J. Fu, and P.X. Do, "State of the art of control schemes for smart systems featuring magneto-rheological materials," *Smart Mater. Struct.*, vol. 25, no. 4, p. 043001, 2016, doi:10.1088/0964-1726/25/4/043001.
- [13] M. -S. Seong, S.-B. Choi and K.-G. Sung, "Control Strategies for Vehicle Suspension System Featuring Magnetorheological (MR) Damper," in *Vibration Analysis and Control - New Trends and Developments*. London, United Kingdom: IntechOpen, 2011 [Online]. Available: <https://www.intechopen.com/chapters/17687> doi: 10.5772/24556.
- [14] K. E. Majdoub, F. Giri and F. -Z. Chaoui, "Adaptive Backstepping Control Design for Semi-Active Suspension of Half-Vehicle with Magnetorheological Damper," *IEEE/CAA Journal of Automatica Sinica*, vol. 8, no. 3, pp. 582-596, March 2021, doi: 10.1109/JAS.2020.1003521.
- [15] P. Hui, C. Jia-nan, and L. Kai, "Adaptive Backstepping Tracking Control for Vehicle Semi-active Suspension System with Magnetorheological Damper," *Acta Armamentarii*, vol. 38, no. 7, pp. 1430-1442. 2017, doi: 10.3969/j.issn.1000-1093.2017.07.023.
- [16] K. El Majdoub and H. Ouadi, "Backstepping Control for Semi-Active Suspension of Half-Vehicle with Dahl Magnetorheological Damper Model," *International Journal on Engineering Applications (IREA)*, vol. 3, no. 4, pp. 96-107, 2015.
- [17] L. I. Nkomo, O. T. Nyandoro, and A. Dove, "Comparison of Backstepping and Sliding Mode Control Techniques for A High Performance Active Vehicle Suspension System," *IFAC-PapersOnLine*, vol.50, no. 1, pp. 12604-12610, 2017, doi: 10.1016/j.ifacol.2017.08.2202.
- [18] S. Fazeliand A. Moarefianpur, "An adaptive approach for vehicle suspension system control in presence of uncertainty and unknown actuator time delay," *Systems Science & Control Engineering*, vol. 9, no. 1, pp.117-126,2021, doi:10.1080/21642583.20201850369.
- [19] H. Pang, X. Zhang, J. Yang, and Y. Shang, "Adaptive backstepping-based control design for uncertain nonlinear active suspension system with input delay," *International Journal of Robust and Nonlinear Control*, vol. 29, no. 16, pp. 5781–5800. 2019, doi: 10.1002/rnc.4695.
- [20] R. Bai and D. Guo, "Sliding-Mode Control of the Active Suspension System with the Dynamics of a Hydraulic Actuator," *Complexity*, vol. 2018, p. 5907208, 2018, doi:10.1155/2018/5907208.
- [21] C. Yang, J. Xia, J. H. Park, H. Shen, and J. Wang, "Sliding mode control for uncertain active vehicle suspension systems: an event-triggered  $H_\infty$  control scheme," *Nonlinear Dynamics*, vol. 103, pp. 3209–3221. 2021, doi: 10.1007/s11071-020-05742-z.
- [22] A. J. Koshkouei and K. J. Burnham, "Sliding Mode Controllers for Active Suspensions," *IFAC Proceedings Volumes*, vol. 41, no. 2, pp. 3416-3421, 2008, doi:10.3182/20080706-5-KR-1001.00580.
- [23] L. M. Jansen and S. J. Dyke, "Semiactive control strategies for MR Dampers: Comparative study," *Journal of Engineering Mechanics*, vol. 126, no. 8, pp. 795-803, 2000, doi:10.1061/(asce)0733-9399(200)126:8(795).
- [24] S. J. Dyke, B. F. Jr. Spencer, M. K. Sain, and J. D. Carlson, "An experimental study of MR dampers for seismic protection," *Journal of Smart Material and Structure*, vol. 7, no. 5, pp. 693–703. 1998, doi:10.1088/0964-1726/7/5/012.
- [25] Y. Kim, R. Langari, S. Hurlebaus, "Semi active nonlinear control of a building with a magnetorheological damper system," *Mechanical Systems and Signal Processing*, vol. 23, no. 2, pp. 300–315, 2009, doi: 10.1016/j.ymsp.2008.06.006.
- [26] A. M. Aly, "Vibration Control of Buildings Using Magnetorheological Damper: A New Control Algorithm," *Journal of Engineering*, vol. 2013, p. 596078, 2013, doi:10.1155/2013/596078.
- [27] A. Bathaei, S. M. Zahrai, and M. Ramezani "Semi-active seismic control of an 11-DOFbuilding model with TMD + MR damper using type-1 and-2 fuzzy algorithms," *Journal of Vibration and Control*, vol. 24, pp. 2938–2953, 2018, doi: 10.1177/1077546317696369.
- [28] X. Lin, S. Chen, and G. Huang, "A shuffled frog-leaping algorithm based mixed-sensitivity  $H_\infty$  control of a seismicallyexcited structural building using MR dampers," *Journal of Vibration and Control*, vol. 24: pp. 2832–2852, 2018, doi: 10.1177/1077546317695462.
- [29] B.F. Jr. Spencer, S. D. Dyke, M. K. Sain, and J. D. Carlson, "Phenomenological model for Magneto-Rheological Dampers," *Journal of Engineering Mechanics*, vol. 123, no. 3, pp. 230-238, 1997, doi: 10.1177/1077546317695462.
- [30] L.-H. Zong, X.-L. Gong, C. -Y. Guo, and S.-H. Xuan, "Inverse neuro-fuzzy MR damper model and its application in vibration control of vehicle suspension system," *Vehicle System Dynamics*, vol. 50, no. 7, pp. 1025-1041, 2012, doi: 10.1080/00423114.2011.645489.
- [31] S.J. Dyke, B. F. Jr. Spencer, M. K. Sain, and J. D. Carlson, "Modeling and control of magnetorheological dampers for seismic response reduction," *Smart Materials and Structures*, vol. 5, no. 5, pp. 565–575, 1996, doi:10.1088/0964-1726/5/5/006.
- [32] S. Dutta and S.B. Choi, "A nonlinear kinematic and dynamic modeling of Macpherson suspension systems with a magneto-rheological damper," *Smart Materials and Structures*, vol. 25, no. 3, p. 035003. 2016, doi: 10.1088/0964-1726/25/3/035003.
- [33] M. Krstic, I. Kanellakopoulos, and P. V. Kokotovic, "Nonlinear design of adaptive controllers for linear systems," *IEEE Transactions on Automatic Control*, vol. 39, no. 4, pp. 738-752, April 1994, doi: 10.1109/9.286250.
- [34] K. Z.Meguenni, M. Tahar, M. R. Benhadria, and Y. Bestaoui "Fuzzy integral sliding modebased on backstepping control synthesis for an autonomous helicopter," *Proceedings of the Institutionof Mechanical Engineers, Journal of Aerospace Engineering*, vol. 227, no. 5, pp.751-765, May2013,doi:10.1177/0954410012442119.
- [35] J. Zhang, S. Wang, P. Zhou, L. Zhao, and S. Li, "Novel prescribed performance-tangent barrier Lyapunov function for neural adaptive control of the chaotic PMSM system by backstepping," *International Journal of Electrical Power & Energy Systems*, vol. 121, p. 105991, 2020, doi: 10.1016/j.ijepes.2020.105991.
- [36] Jung-Shan Lin and I. Kanellakopoulos, "Nonlinear design of active suspensions," *IEEE Control Systems Magazine*, vol. 17, no. 3, pp. 45-59, June 1997, doi: 10.1109/37.588129.
- [37] J. Wang, R. Li, G. Zhang, P. Wang, S. Guo, "Continuous sliding mode iterative learning control for output constrained MIMO nonlinear systems," *Information Sciences*, vol. 556, pp. 288-304, 2021, doi: 10.1016/j.ins.2020.12.003
- [38] Q. Wu, X. Wang, L. Hua, and M. Xia, "Modeling and nonlinear sliding mode controls of double pendulum cranes considering distributed mass beams, varying roped length and external disturbances," *Mechanical Systems and Signal Processing*, vol. 158, p. 107756. 2021, doi: 10.1016/j.ymsp.2021.107756.
- [39] M. Spiller and D. Söffker, "Chattering mitigated sliding mode control of uncertain nonlinear systems," *IFAC-PapersOnLine*, vol. 53, no. 2,pp. 6244-6249, 2020, doi:10.1016/j.ifacol.2020.12.1734.
- [40] G. Ram and Santha K R, "Review of Sliding Mode Observers for Sensorless Control of Permanent Magnet Synchronous Motor Drives," *Int. J. Power Electron. Drive Syst.*, vol. 9, no. 1, pp. 46-54, 2018, 10.11591/ijpeds.v9.i1.pp46-54.
- [41] A. Omari, I. K. Bousserhane, A. Hazzab, and B. Bouchiba, "dSPACE DS1104 Based Real Time Implementation of Sliding Mode Control of Induction Motor," *Int. J. Power Electron. Drive Syst.*,vol. 9, no. 2, pp. 546-558, 2018, doi: 10.11591/ijpeds.v9.i2.pp546-558.
- [42] S.Miqoi, A. E. Ogli, and B. Tidhaf, "Adaptive fuzzy sliding mode based MPPT controller for a photovoltaic water pumping system," *Int. J. Power Electron. Drive Syst.*, vol. 10, no. 1, pp. 414-422, 2019, doi: 10.11591/ijpeds.v10.i1.pp414-422.




- [43] H. Alami Aroussi, El. M. Ziani, M. Bouderbala, B. Bossoufi, "Improvement of Direct Torque Control Applied to Doubly Fed Induction Motor Under Variable Speed," *International Journal of Power Electronics and Drive System*, vol. 11, no. 1, pp. 97-106, 2020, doi: 10.11591/ijpeds.v11.i1.pp97-106.
- [44] N. El Ouanjli, A. Derouich, A. El Ghzizal, Y. El Mourabit, M. Taoussi, and B. Bossoufi, "Contribution to the Performance Improvement of Doubly Fed Induction Machine Functioning in Motor Mode by the DTC Control," *International Journal of Power Electronics and Drive System*, vol. 8, no. 3, pp. 1117-1127, 2017, doi: 10.11591/ijpeds.v8.i3.pp1117-1127.
- [45] J. Li, Z. Liu, and Q. Su, "Improved adaptive backstepping sliding mode control for a three-phase PWM AC-DC converter," *IET Control Theory and Applications*, vol. 13, pp. 854-860, 2019, doi:10.1049/iet-cta.2018.5453.
- [46] S. I. Han and J. M. Lee, "Backstepping sliding mode control with FWNN for strict output feedback non-smooth nonlinear dynamic system," *International Journal of Control Automation and Systems*, vol. 11, pp. 398-409, 2013, doi:10.1007/s12555-012-9115-3.
- [47] R. Coban, "Backstepping integral sliding mode control of an electromechanical system," *Automatika*, vol. 58, no. 3, pp. 266-272, 2017, doi: 10.1080/00051144.2018.1426263.
- [48] T. Espinoza, A. Dzul, R. Lozano and P. Parada, "Backstepping — Sliding mode controllers applied to a fixed-wing UAV," *2013 International Conference on Unmanned Aircraft Systems (ICUAS)*, 2013, pp. 95-104, doi: 10.1109/ICUAS.2013.6564678.
- [49] J. Li, Z. Liu, and Q. Su, "Improved adaptive backstepping sliding mode control for a three-phase PWM AC-DC converter," *IET Control Theory and Applications*, vol. 13, pp. 854-860, 2019, doi:10.1049/iet-cta.2018.5453.

## BIOGRAPHIES OF AUTHORS






**Mohamed Belkacem**    received the state engineer degree in electronics in 1996 from the University Djillali LIABES Sidi-Bel-Abbès Algeria. he received his Magister in electrical engineering in 2014 from the University of Science and Technology-Mohamed Boudiaf (USTO), Oran, Algeria. He is currently working toward the doctoral degree. His research interests are in the field of electronics and modern control techniques and their application in the control of nonlinear systems. He can be contacted at email: belkacem\_mohamed03@yahoo.fr



**Kadda Zermalache Meguenni**    received his B.S degree and the M.S degree in Electrical Engineering from University of Sciences and Technology of Oran, Algeria, in 1998, and 2001 respectively and his PhD in Electrical Engineering from University of Evry Val d'Essonne, France, in 2006. He is currently working as an Associate Professor in the Faculty of Electrical Engineering at the University of Sciences and Technology in the city of Oran in Algeria. His research and teaching interests include: Intelligent control, Mechatronics systems and Robotics control. He can be contacted at email: zermalache@hotmail.com



**Ismail Khalil Bousserhane**    received his BS degree in electrical engineering from the Electrical Engineering Institute of the University Center of Bechar in 2000, the M.S. degree and the PhD degree in Electrical Engineering from the University of Sciences and Technology of Oran (Algeria), in 2003 and 2008, respectively. He is currently Professor of electrical engineering at University Tahri Mohamed of Bechar, Algeria. His areas of interest are modern control techniques and their application in electric drives control. He can be contacted at email: bou\_isma@yahoo.fr